Journal of Cancer Research and Clinical Oncology (2025) 151:96
https://doi.org/10.1007/s00432-025-06144-7

RESEARCH

CENPF as a prognostic marker of glioma: unraveling the molecular mechanisms

Xiuyang Chen[1] · Yiwei Wu[2] · Yining Xing[1,2] · Peng Zhong[1]

Received: 21 January 2025 / Accepted: 17 February 2025 / Published online: 28 February 2025

Abstract

Objective Glioma is the dominant primary intracranial malignancy. The roles of CENPF and the CENPF - p53 axis in glioma remain elusive. This study uses bioinformatics and animal experiments to clarify the relationship between CENPF and p53 in glioma. CENPF affects spindle assembly and chromosomal segregation, while p53 is a tumor—suppressor gene. Their dysregulation may interact and impact glioma development. Our research aims to uncover the underlying molecular mechanisms, offering new perspectives for glioma diagnosis and treatment.

Method Gene expression data from the Gene Expression Omnibus (GEO) database (http://www.ncbi.nlm.nih.gov/geo/) were retrieved, specifically datasets GSE50161, GSE104291, and GSE12249. Volcano plots were generated to visualize differentially expressed genes (DEGs), and intersecting DEGs were identified using Venn diagrams. Weighted gene co-expression network analysis (WGCNA) was employed to construct and analyze the protein–protein interaction (PPI) network. Additionally, gene ontology (GO) and Kyoto Encyclopedia of Genes and Genomes (KEGG) pathway analyses were conducted. Gene set enrichment analysis (GSEA) was utilized for comprehensive GO and KEGG analyses of the entire genome. Comparative Toxicogenomics Database (CTD) analysis was performed, and TargetScan was used to identify miRNAs regulating central DEGs. An animal model of glioma was established and analyzed via Western blot.

Result A total of 501 differentially expressed genes (DEGs) were identified, from which eight significant modules were generated and ten core genes were extracted. These core genes exhibited differential expression patterns between glioma tumor and non-tumor samples. Expression analysis revealed that the ten core genes associated with glioma (CENPF, PBK, ASPM, KIF2C, KIF20A, CDC20, TOP2A, NUSAP1, TTK, KIF23) were significantly upregulated in tumor tissues ($P < 0.05$). They are primarily enriched in protein signal transduction, coated membrane structures, AP-type membrane coat adaptor complexes, and chloride channel activity. KEGG pathway analysis indicated that these target genes were mainly involved in nicotine addiction, arginine and proline metabolism, beta-alanine metabolism, and histidine metabolism. The mouse model confirmed that CENPF and CDK-1 were highly expressed in glioma tissues, while p53, p21, and Caspase9 were downregulated, leading to inhibition of the apoptosis pathway and exacerbation of glioma progression. Overexpression of CENPF further suppressed key molecules in the p53-mediated apoptosis pathway. Conversely, low expression of CENPF activated these key molecules, inducing apoptosis in glioma cells.

Conclusions CENPF exhibits elevated expression levels in glioma, potentially inhibiting cell apoptosis via the p53 signaling pathway, consequently contributing to the onset and progression of glioma.

Keywords Glioma · CENPF · P53 · Prognostic markers · Differentially expressed genes (DEGs)

Introduction

Glioma, the most common primary intracranial neoplasm originating from glial cells, is a major health concern due to its high incidence, recurrence, and mortality rates, along with low remission rates (Gusyatiner and Hegi 2018). Its presence in various brain locations gives rise to a wide range of symptoms (Norouzi 2020), including hemorrhage, limb

✉ Peng Zhong
drzhongpeng@163.com

[1] Department of Neurological Care Unit, The Affliated Yantai Yuhuangding Hospital of Qingdao University, No. 20, Yuhuangding East Road, Zhifu District, Yantai 264000, Shandong, People's Republic of China

[2] Department of Orthopaedic Surgery, Yantaishan Hospital, Yantai 264000, Shandong, People's Republic of China

paralysis, cognitive impairment, epilepsy, and blindness, severely deteriorating patients' quality of life and threatening their survival (Tsitlakidis et al. 2020; Xu et al. 2020).

Current treatment strategies for glioma, such as surgical resection, radiation therapy, chemotherapy, and targeted therapies, require a comprehensive assessment of multiple factors like patient functional status, expected treatment outcomes, tumor location, and malignancy grade to formulate an individualized treatment plan (Ellert-Miklaszewska et al. 2020). However, the etiology of glioma remains unclear, with potential links to genetic factors, chromosomal aberrations, and gene fusions. Thus, understanding the molecular mechanisms underlying glioma development is crucial.

Genes play a pivotal role in glioma progression. CENPF (Centromere Protein F) is a nuclear—localized protein associated with the centromere and kinetochore complex (Li et al. 2020). It is involved in spindle assembly and chromosomal segregation during mitosis. When CENPF is misregulated, it can lead to genomic instability, a common characteristic in glioma cells (Hur et al. 2019).

The p53 gene, located on human chromosome 17 at position p13, is a well-known tumor-suppressor gene (Sabapathy and Lane 2019). It encodes a phosphoprotein that plays a central role in cell-cycle control, DNA repair, and apoptosis. The p53 protein, existing as a tetramer in vivo, is crucial for maintaining normal cellular activities (Liu et al. 2019). Its DNA-binding domain has endonuclease activity, influencing DNA recombination and repair (Agupitan et al. 2020).

The reason for studying CENPF and p53 in relation to glioma is their fundamental roles in cellular processes that are often dysregulated in cancer. CENPF's role in maintaining chromosomal stability and p53's function in tumor suppression are likely interconnected. For example, genomic instability caused by CENPF misregulation could potentially disrupt the normal functions of p53. When CENPF-induced chromosomal abnormalities occur, p53's ability to regulate the cell cycle and initiate DNA repair or apoptosis might be compromised. Conversely, defects in p53 could also affect the normal regulation of CENPF, leading to further genomic instability (Sun et al. 2023). Understanding this relationship could provide new insights into the complex molecular mechanisms driving glioma development.

In modern biological research, bioinformatics technology has become an essential tool. It involves processing and analyzing diverse proteomic data, and its scope has expanded from basic genome and proteome analysis to exploring known and novel gene products (Fu et al. 2020; Chen et al. 2020).

This study aims to use bioinformatics methods to identify core genes differentiating glioma from normal tissues and conduct enrichment and pathway analyses. The significant roles of p53 and CENPF in glioma were validated using public datasets and further confirmed through fundamental cellular experiments. To ensure consistency, the abstract will be updated to clearly state the focus on p53 and CENPF in the context of glioma research.

Methods

Data source and sample information

Glioma brain-tumor datasets GSE104291, GSE122498, and their corresponding configuration files were retrieved from the GPL570 GEO database (http://www.ncbi.nlm.nih.gov/geo/). GSE50161 encompassed 34 glioma tumor samples and 13 non-tumor brain tissue samples. GSE104291 consisted of 4 glioma tumor samples and 2 non-tumor brain tissue samples, while GSE122498 contained 16 glioma tumor samples. These datasets were utilized to identify differentially expressed genes (DEGs) for glioma tumor analysis.

Data analysis

Screening of DEGs

For the matrices of GSE50161, GSE104291, and GSE122498, the R package "limma" was employed to conduct probe summarization and background correction separately. Differential gene screening was based on matrix score, immune score, and disease status. The Benjamini-Hochberg method was utilized to adjust the raw P-values, and the fold-change (FC) was calculated using the false discovery rate (FDR). The criterion for identifying DEGs was set as $FDR < 0.05$. Subsequently, a volcano plot was generated to visualize the differential genes, and the intersection of DEGs was obtained through a Venn diagram.

Weighted gene co—expression network analysis (WGCNA)

The Median Absolute Deviation (MAD) of each gene was computed individually using the GSE50161, GSE104291, and GSE122498 matrices. The top 50% of genes with the lowest MAD values were excluded. Outlier genes and samples were eliminated via the goodSamplesGenes method within the R software package WGCNA. A scale-free co-expression network was constructed as follows: First, for all gene pairs, the Pearson correlation matrix was calculated and the average chain method was applied. Then, the power function (where represents the Pearson correlation between Gene and Gene, and represents the adjacency between Gene and Gene) with was used to construct the weighted adjacency matrix. This adjacency matrix was then converted into a topological overlap matrix (TOM). TOM quantifies the network connectivity of a gene, which is defined as the sum of its connections with all other genes in the network

relative to the total number of genes. Concurrently, the corresponding degree of dissimilarity (1-TOM) was computed. To cluster genes with comparable expression profiles into gene modules, average linkage hierarchical clustering was implemented based on the dissimilarity measures derived from TOM. The minimum size of the gene dendrogram was set at 30, and the sensitivity was adjusted to 3. For a more in-depth module analysis, the dissimilarity of module-characteristic genes was determined. Subsequently, a cutoff line for the module dendrogram was chosen, and modules with a distance less than 0.25 were merged. Eventually, 16 co-expression modules were acquired. Grey modules were regarded as gene sets that could not be allocated to any particular module.

Construction and analysis of protein–protein interaction (PPI) network

The STRING database (https://string-db.org/) was used to construct a protein–protein interaction (PPI) network. The list of differential genes was input into the STRING database to identify core genes with a confidence level greater than 0.4. Cytoscape software was utilized to visualize the PPI network generated by the STRING database. After importing the PPI network into Cytoscape software, the module with the highest correlation was located using MCODE. Subsequently, two algorithms, Maximal Clique Centrality (MCC) and Maximum Neighborhood Component (MNC), were employed to calculate the ten genes with the strongest correlations and determine their intersection. Finally, the core gene list was obtained, providing valuable information for further investigation (Fig. 1B).

Functional enrichment analysis

Gene Ontology (GO) analysis and Kyoto Encyclopedia of Genes and Genomes (KEGG) analysis were performed to assess gene functions and biological pathways. The differences in the gene list were input into the KEGG rest API (https://www.kegg.jp/kegg/rest/keggapi.html) to retrieve the latest KEGG Pathway gene annotations, which served as the background for mapping the genes to the collection. The R package clusterProfiler (version 3.14.3) was utilized for enrichment analysis to obtain the gene set enrichment results. In addition, the GO annotations of genes in the R package org.Hs.eg.db (version 3.1.0) were also used as the background. The genes were mapped to the background set with a minimum gene set of 5 and a maximum gene set of 5000. A P-value less than 0.05 and a false discovery rate (FDR) less than 0.25 were regarded as statistically significant measures.

Furthermore, the Metascape database (http://metascape.org/gp/index.html) was employed to conduct functional analysis of the gene enrichment differences and export the list.

Gene set enrichment analysis (GSEA)

Gene set enrichment analysis (GSEA) was carried out to conduct GO and KEGG analyses on the whole genome. Whole-blood samples were categorized based on pre-exercise and post-exercise conditions, and then whole-genome GO and KEGG analyses were executed using the GSEA technique.

Heat map of gene expression

The R package "heatmap" was used to generate heat maps depicting the expression levels of the core genes identified by the MCC and MNC algorithms within the PPI networks of GSE50161, GSE104291, and GSE122498. These heat maps were utilized to visually represent the expression differences of the core genes between glioma tumor and non-tumor samples.

Other analyses

1. **CTD Analysis:** The Comparative Toxicogenomics Database (CTD) was used. The core genes were input into the CTD website, and the diseases most closely associated with the 10 core genes were identified and presented in the form of radar charts.
2. **miRNA Analysis:** The online database TargetScan (www.targetscan.org) was employed to screen for microRNAs (miRNAs) that regulate the key differentially expressed genes (DEGs).
3. **Establishment of mouse animal model:** C57BL/6 mice at 8 ± 1 weeks of age were weighed and the weights were recorded. Subsequently, they were numbered and randomly assigned to groups using the random number table method. The mice were divided into 4 groups, with 6 mice in each group: Group A (control), Group B (GBM), Group C (GBM/CENPF overexpression), and Group D (GBM/CENPF knockout). To establish the orthotopic xenograft model of glioma, tumor cell suspension was inoculated into the mice. On a super-clean bench, the mice were anesthetized by intraperitoneal injection of 1% barbital (0.01 ml/g), and a cotton ball soaked with a small amount of ether was placed in front of their noses for additional anesthesia. After routine disinfection, the injection site was determined, and 6 µl of the tumor cell suspension was slowly aspirated vertically into the brain parenchyma of the mice using a 50-µl microsyringe. After gentle injection, the needle was held in place for 5 min. Then, the needle was slowly withdrawn, sterilized, and the mice were placed in a spe-

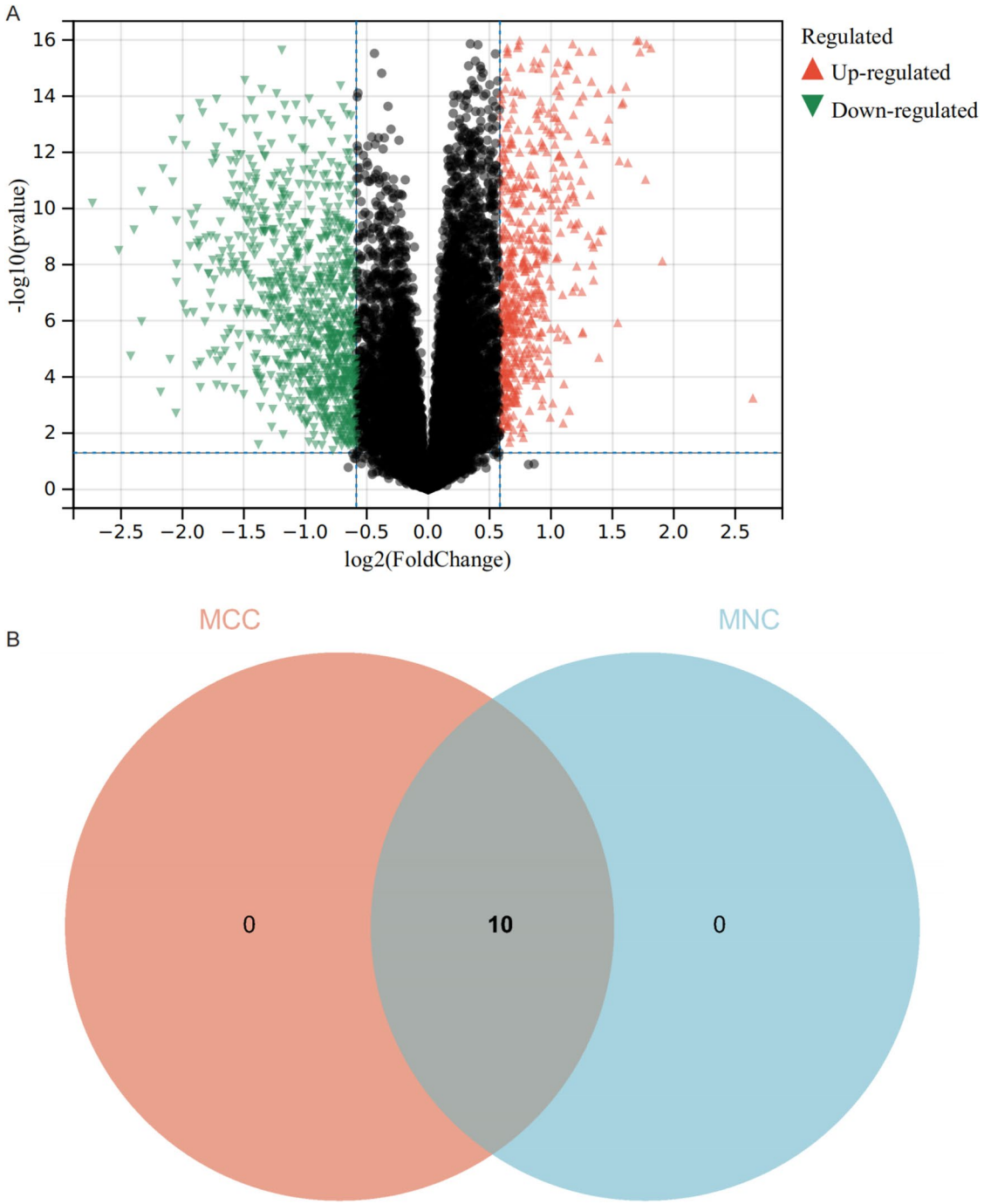

Fig. 1 **A** Functional enrichment analysis of DEGs. A total of 501 DEGs were identified. **B** Maximal Clique Centrality (MCC) and Maximum Neighborhood Component (MNC) algorithms to calculate the top ten most—correlated genes and find their intersection

cific pathogen-free environment. The growth status of the mice was observed and recorded daily.

4. **Immunofluorescence:** The tissue sections were placed in a repair box filled with EDTA antigen-repair buffer (pH 9.0) for antigen repair in a microwave oven. Then, 0.5% triton x-100 was used to permeate the cell membrane at room temperature for 20 min. Thereafter, BSA was added to rinse the tissue for 1 h. These slices were then incubated overnight at 4 °C with anti-CENPF (1:500, Abcam) as the primary antibody. The slices were then washed 3 times in PBS and incubated with Alexa Fluor 488 anti-mouse IgG (1:1000, Invitrogen) for 1 h at room temperature. After washing with PBS again, the slices were incubated with DAPI fluoro-

mount-G (Southernbiotech, USA) followed by the anti-fluorescence quenching agent. Fluorescent microscopy (OLYMPUS-BX51) and the Magna Fire SP system were used to examine and analyze the microphotographs.

5. **Western Blot:** Total protein was extracted from the tissue. Once the concentration was determined by the UV method, 1/4 of the volume of each protein sample was mixed with 5 × protein loading buffer (reduced). The mixtures were then boiled at 100 °C for 10 min, cooled, packaged, and stored frozen at− 80 °C until further use. The protein samples were subjected to 12% SDS—PAGE gel electrophoresis followed by membrane transfer and other procedures. The membranes were blocked with 5% skim milk at room temperature for 1 h. Subsequently, the primary antibody was added and the samples were incubated overnight at 4 °C. After three washes with TBST (5 min each), the rabbit secondary antibody was added. After incubation for 1 h at room temperature, the samples were washed three more times with TBST (5 min each). Finally, the results were analyzed after developing the chemiluminescence solution.

Results

Functional enrichment analysis of DEGs

In the present study, a comprehensive analysis led to the identification of 501 DEGs. These DEGs were pinpointed through the debatching merge matrix of GSE50161, GSE104291, and GSE122498 (Fig. 1A). Subsequently, Gene Ontology (GO) and Kyoto Encyclopedia of Genes and Genomes (KEGG) analyses were conducted on these identified genes. The GO analysis outcomes revealed that they were predominantly enriched in several key biological processes and cellular components, such as ho protein signal transduction, coated membrane, AP-type membrane coat adaptor complex, and chloride channel activity. Meanwhile, the KEGG analysis demonstrated that the target genes were chiefly concentrated in pathways related to nicotine addiction, arginine and proline metabolism, beta-Alanine metabolism, and histidine metabolism (Fig. 2).

WGCNA analysis

In the realm of WGCNA, the determination of the soft threshold power represents a linchpin step. This parameter wields substantial influence over the robustness and interpretability of the ensuing gene co-expression network. To ascertain the optimal soft threshold power, network topology analysis was used to ascertain the optimal soft threshold power. After painstaking calculations and iterative model refinements, a soft threshold power of 9 was determined for this particular WGCNA analysis. Significantly, this value corresponds to the minimal power requisite for achieving a scale-free topological fit index of 0.9, as vividly depicted in (Figs. 3A, B). This strategic choice laid the groundwork for a more reliable and biologically relevant network construction.

Once the soft threshold power was determined, the research proceeded to the next step. All available genes were used as building blocks to meticulously construct a hierarchical clustering tree. This dendrogram served as a blueprint, carving out eight prominent and functionally distinct modules (Fig. 3C). These modules, akin to interconnected hubs within the gene network, were then subjected to an in-depth exploration of their mutual interactions (Fig. 3D). Unraveling these relationships was crucial in deciphering the underlying genetic regulatory mechanisms.

As documented in the seminal work *MERGEFORMAT (Tang et al. 2018), state-of-the-art statistical techniques were employed to compute the expression correlation between module feature vectors and genes, yielding the Module Membership (MM) metric. By applying a stringent cutoff of (|MM|> 0.8), 1909 genes with pronounced connectivity within the clinically relevant modules were identified. These genes, acting as the veritable powerhouses of the network, were aptly designated as hub genes. Their identification not only sheds light on the core regulatory circuitry but also paves the way for future investigations into disease pathogenesis and potential therapeutic interventions.

Construction and analysis of protein–protein interaction (PPI) network

To gain deeper insights into the functional relationships among differentially expressed genes (DEGs), a protein–protein interaction (PPI) network was constructed. A comprehensive PPI network specific to the DEGs under investigation was assembled by utilizing the STRING online database. Subsequently, this network was imported into Cytoscape software for in-depth analysis (Fig. 4A). Two distinct and advanced algorithms were employed in the pursuit of identifying key regulatory elements. These algorithms meticulously sifted through the network's complex architecture, ultimately pinpointing the hub genes (Fig. 4B, C). Through this rigorous process, a set of 10 core genes, which are likely to play central roles in the biological processes under study, were successfully identified.

Metascape enrichment analysis

Metascape, a powerful bioinformatics tool, was harnessed to perform enrichment analysis. The outcomes of this analysis, which encompassed both the pathways and biological processes implicated, are visually presented in Figs. 5 and 6. These figures offer a detailed snapshot of the complex web

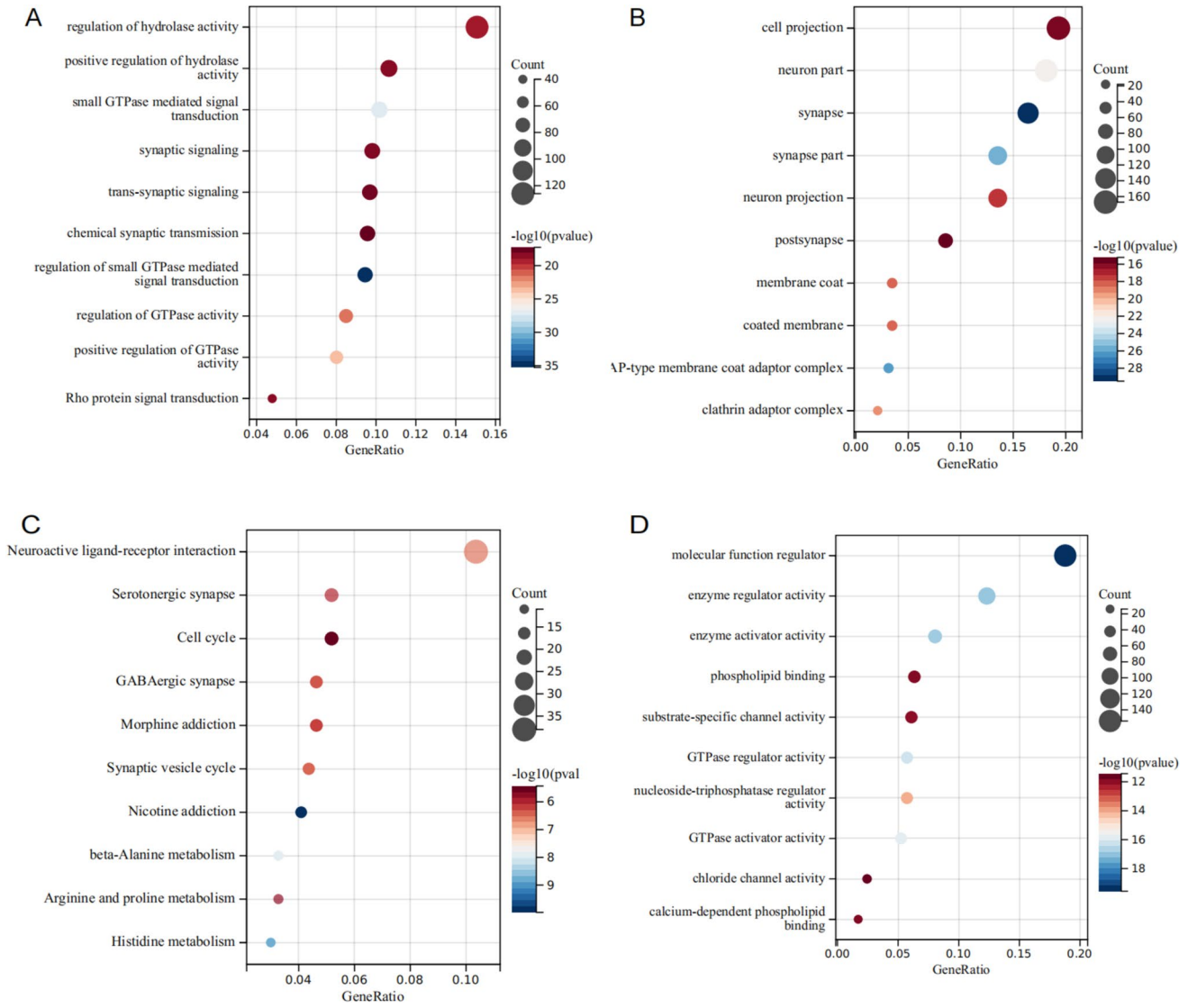

Fig. 2 The differentially expressed genes were analyzed by GO and KEGG. The differentially expressed genes were analyzed by GO and KEGG

of molecular events and cellular functions that the DEGs are involved in, providing crucial clues for further research.

Core gene expression analysis

For the Gene Set Enrichment Analysis (GSEA), the GSEA software (version 3.0) was sourced directly from its official website (DOI: 10.1073 / pnas. 0506580102, http://software.broadinstitute.org/gsea/index.jsp). In this study, samples were meticulously partitioned into two distinct groups, with one group comprising glioma tumor samples and the other consisting of non-tumor samples. To conduct a comprehensive analysis, The c2.cp.kegg.v7.4.symbols.gmt file was further procured from the Molecular Signatures Database (DOI: 10.1093 / bioinformatics/btr260, http://www.gsea-msigdb.org/gsea/downloads.jsp).

This setup enabled us to evaluate the relevant pathways and molecular mechanisms underlying the studied phenomenon. Specifically, based on the gene expression profiling and the predefined phenotype grouping, we established a series of stringent criteria for statistical significance. A minimum gene set size of 5, a maximum gene set size of 5000, along with 1000 rounds of resampling were implemented. Additionally, only those results with a P value less than 0.05 and a false discovery rate (FDR) lower than 0.25 were considered to carry meaningful biological implications (Fig. 7). Through this rigorous Gene Set Enrichment Analysis (GSEA) process, the aim was to unravel the hidden regulatory patterns and gain a more profound understanding of the gene functions within the context of glioma and its associated biological processes.

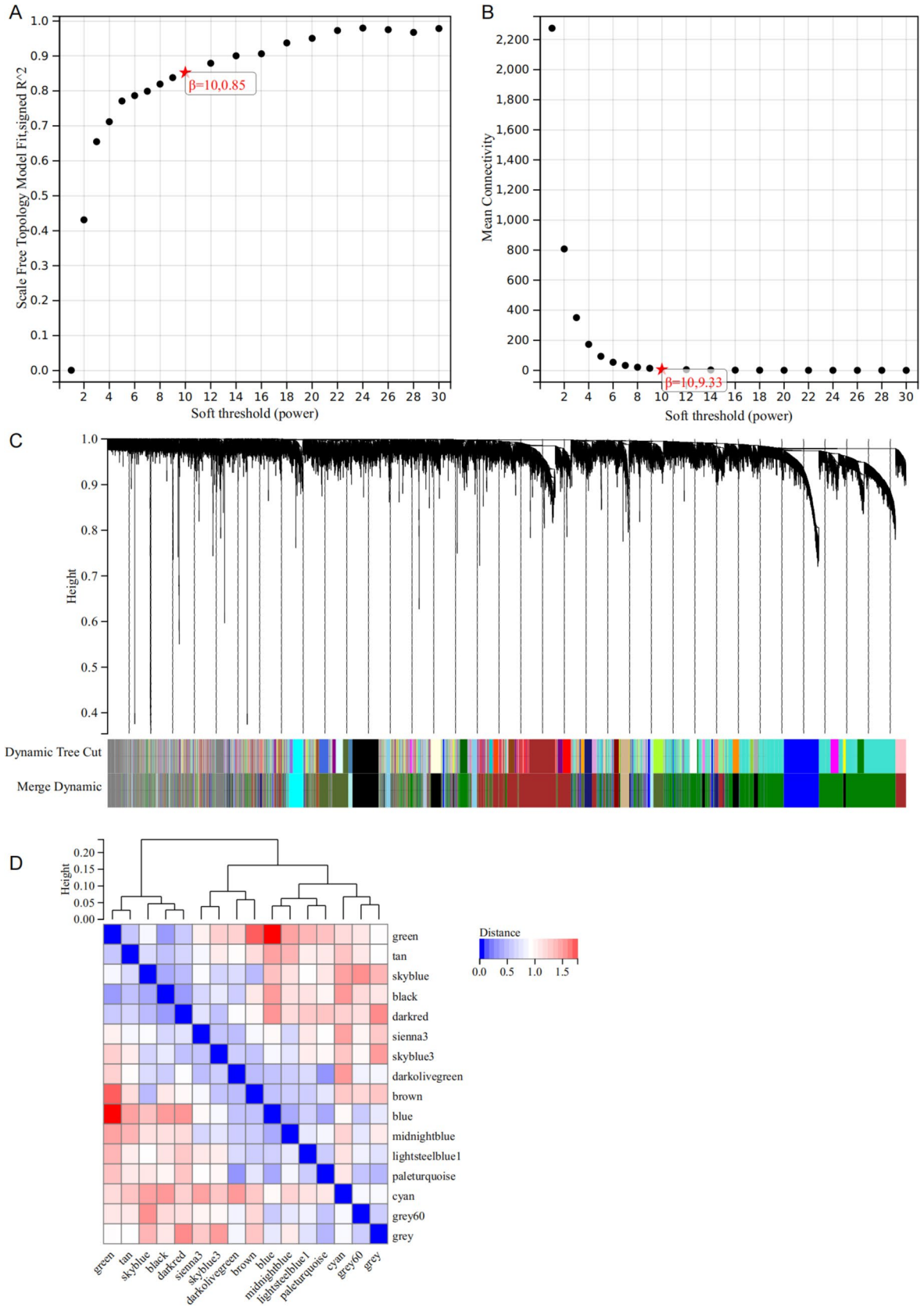

Fig. 3 WGCNA analysis. **A** β = 10,0.85; **B** β = 10,9.33; **C** 8 important modules; **D** Interaction between modules

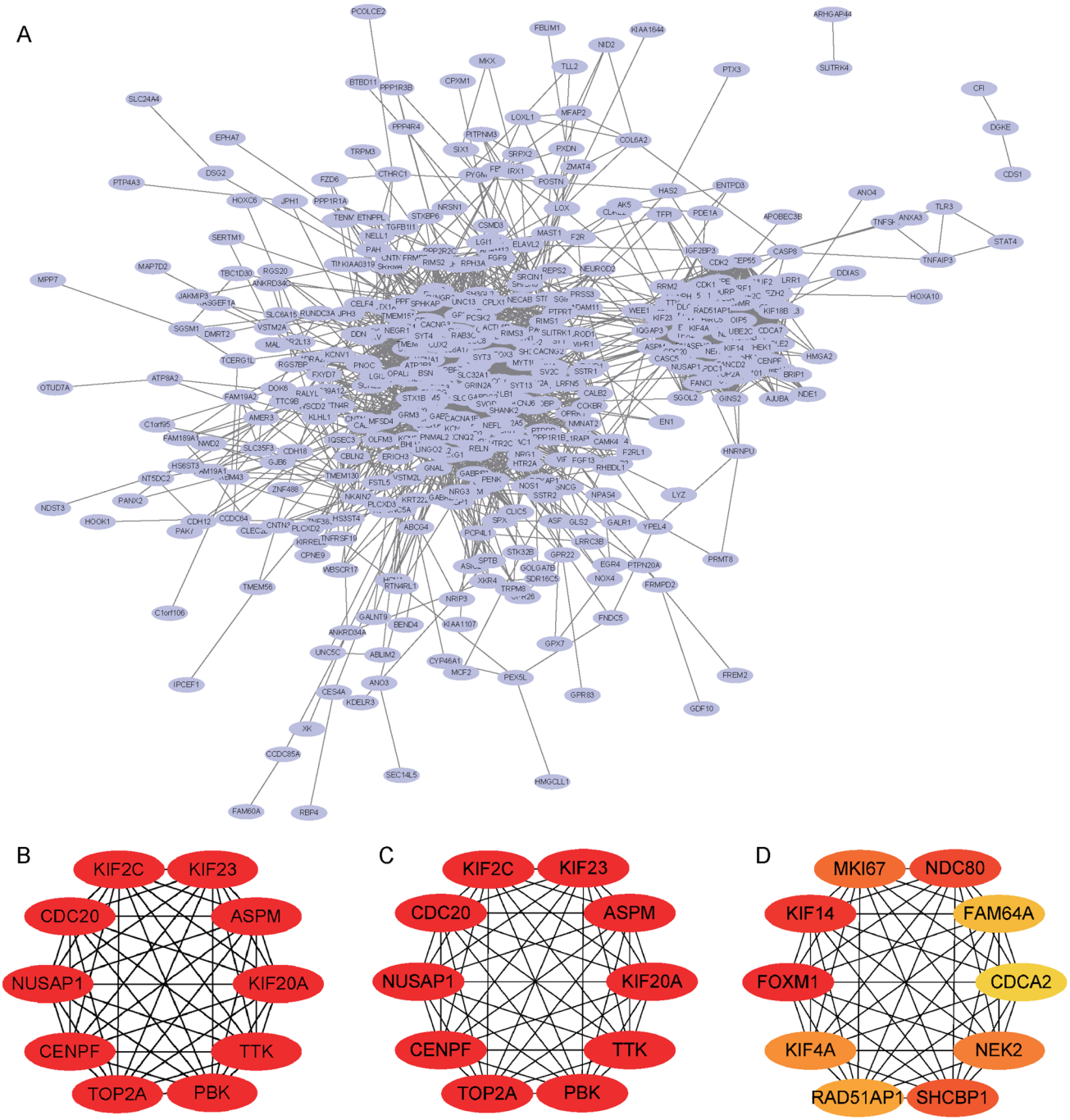

Fig. 4 Construction and analysis of protein–protein interaction (PPI) network. **A** PPI network of DEGs; **B**, **C** 10 core genes

Heat map of gene expression

To understand glioma's molecular differences, the core gene expression was studied. The transcriptional profiles of glioma tumor and non—tumor samples were compared to identify genes with significant expression differences. This helps explain glioma development and find biomarkers or targets.

Expression data was analyzed using advanced techniques and tools. Figure 8 shows clear differences in some core genes. These genes may be key in cell processes like proliferation, apoptosis, and angiogenesis, linked to glioma. Studying their differential expression could clarify glioma biology and lead to better diagnostics and treatments.

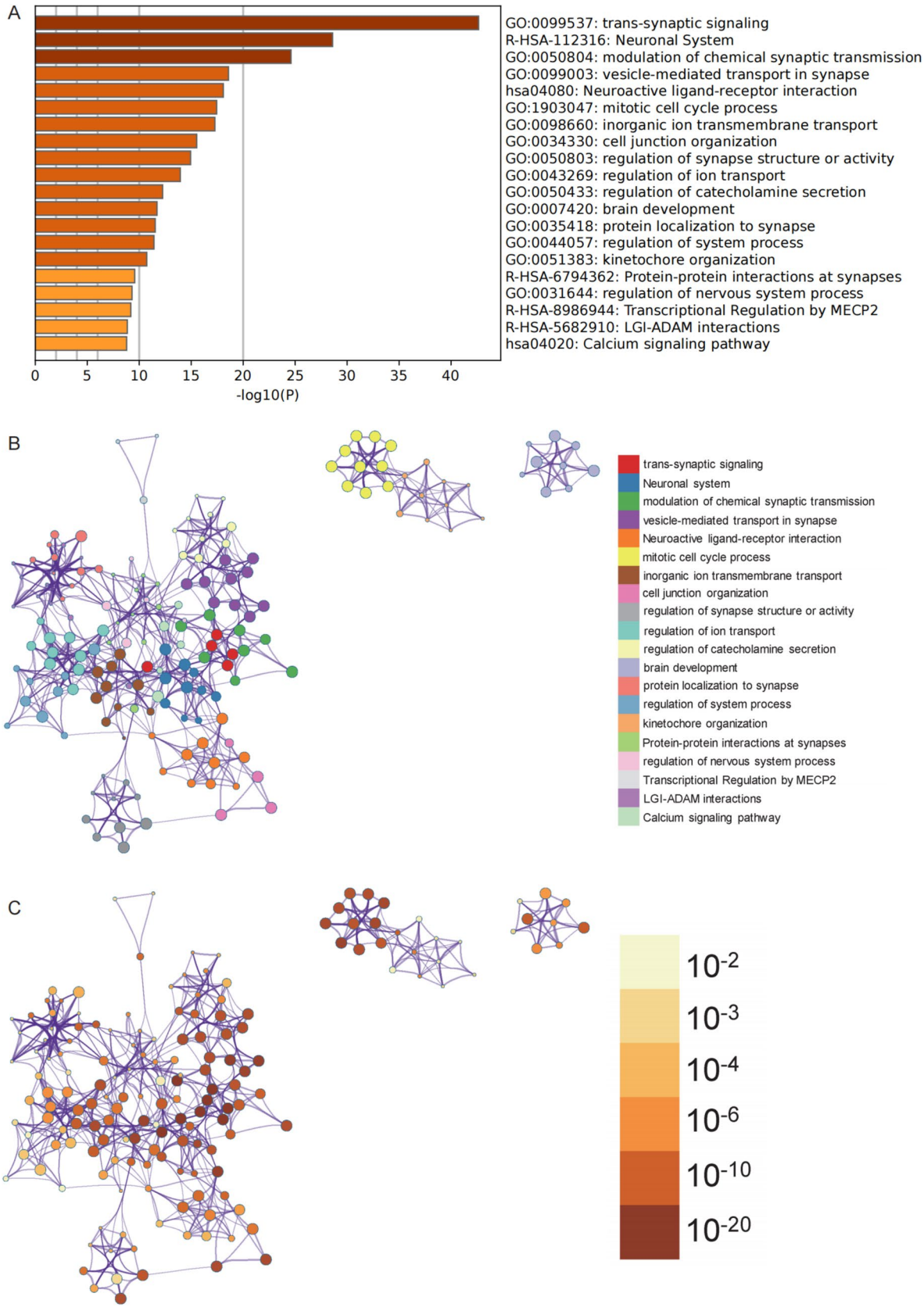

Fig. 5 Pathways and processes for Metascape enrichment analysis

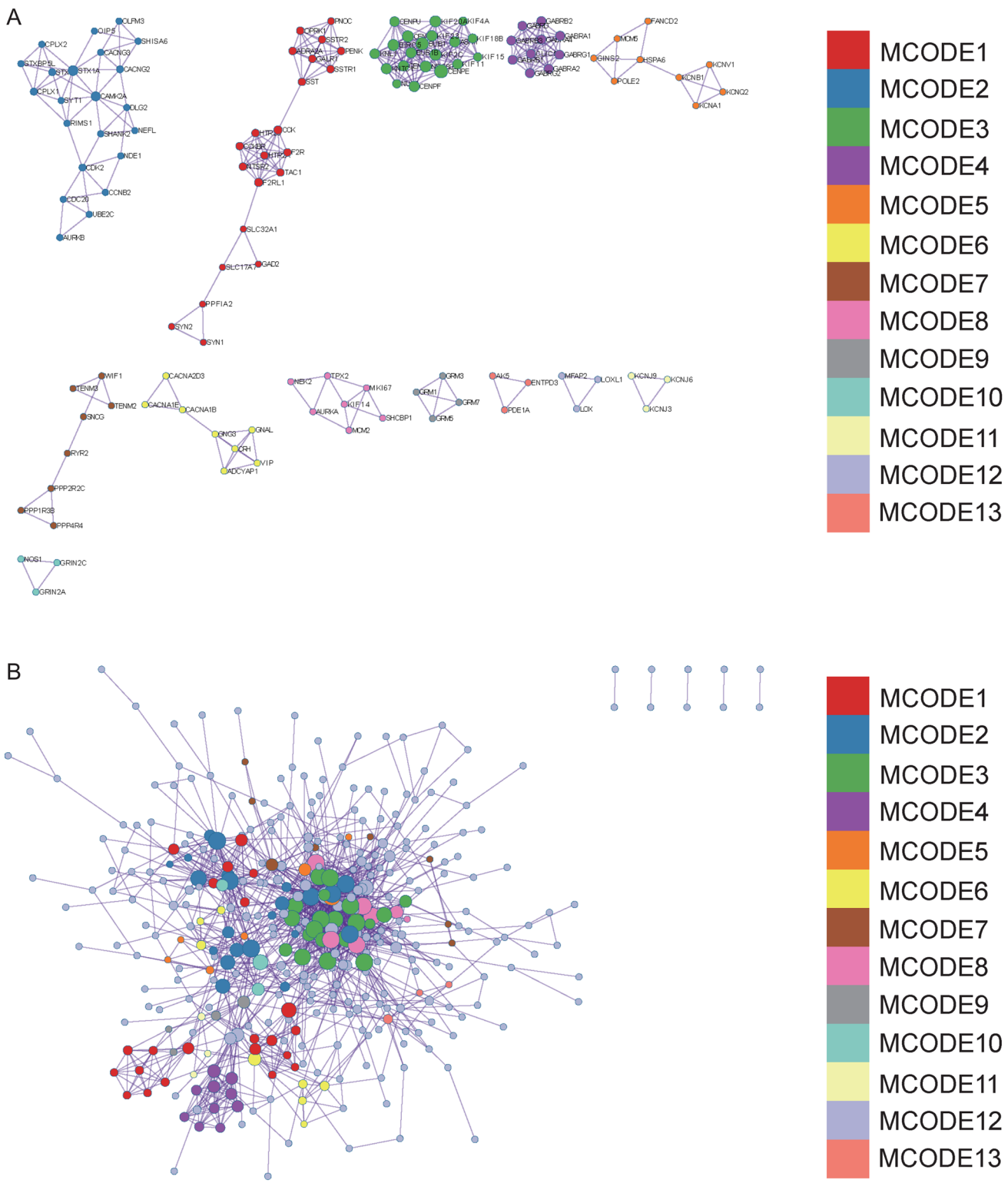

Fig. 6 Results of the Metascape enrichment analysis

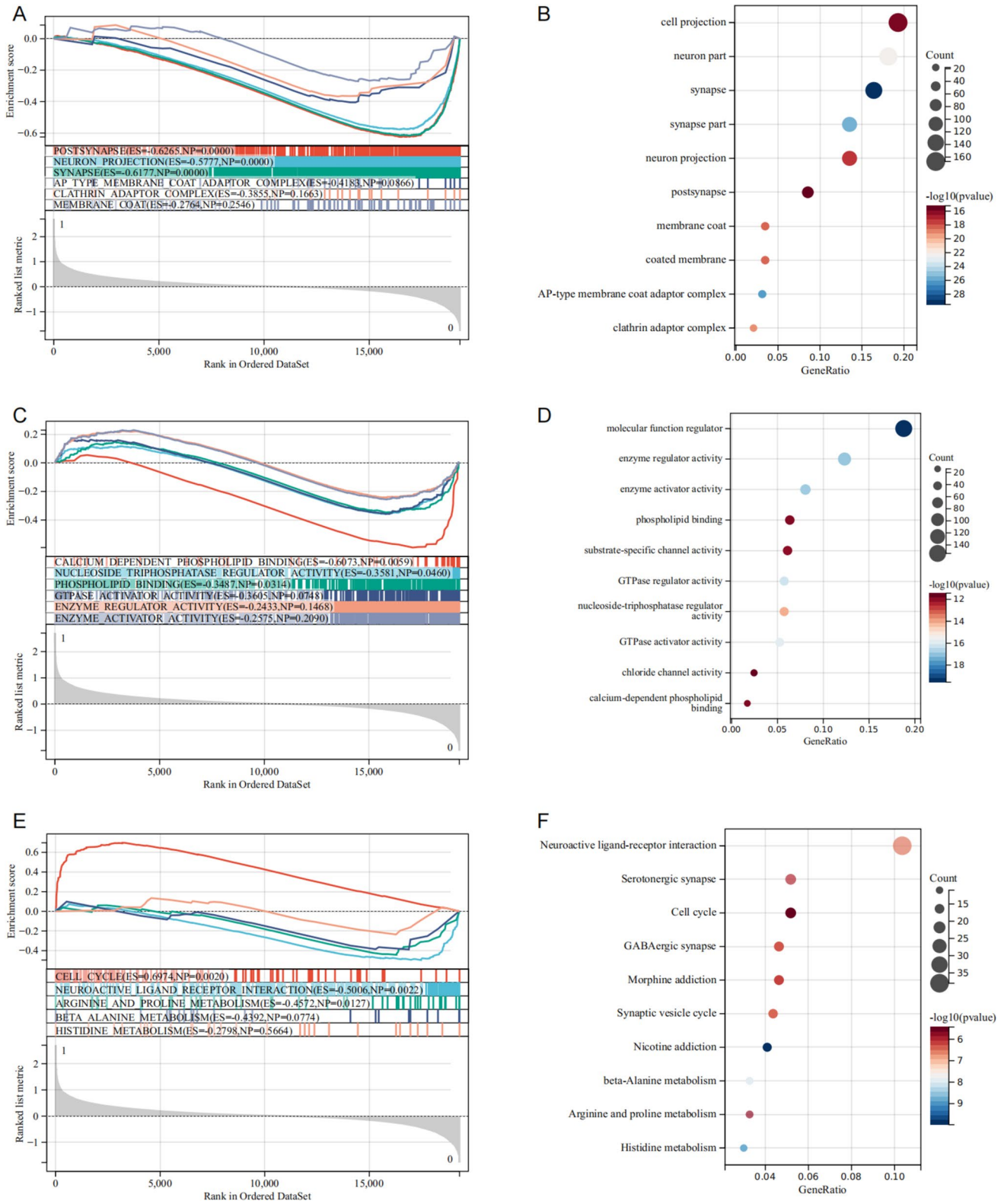

Fig. 7 GSEA analysis

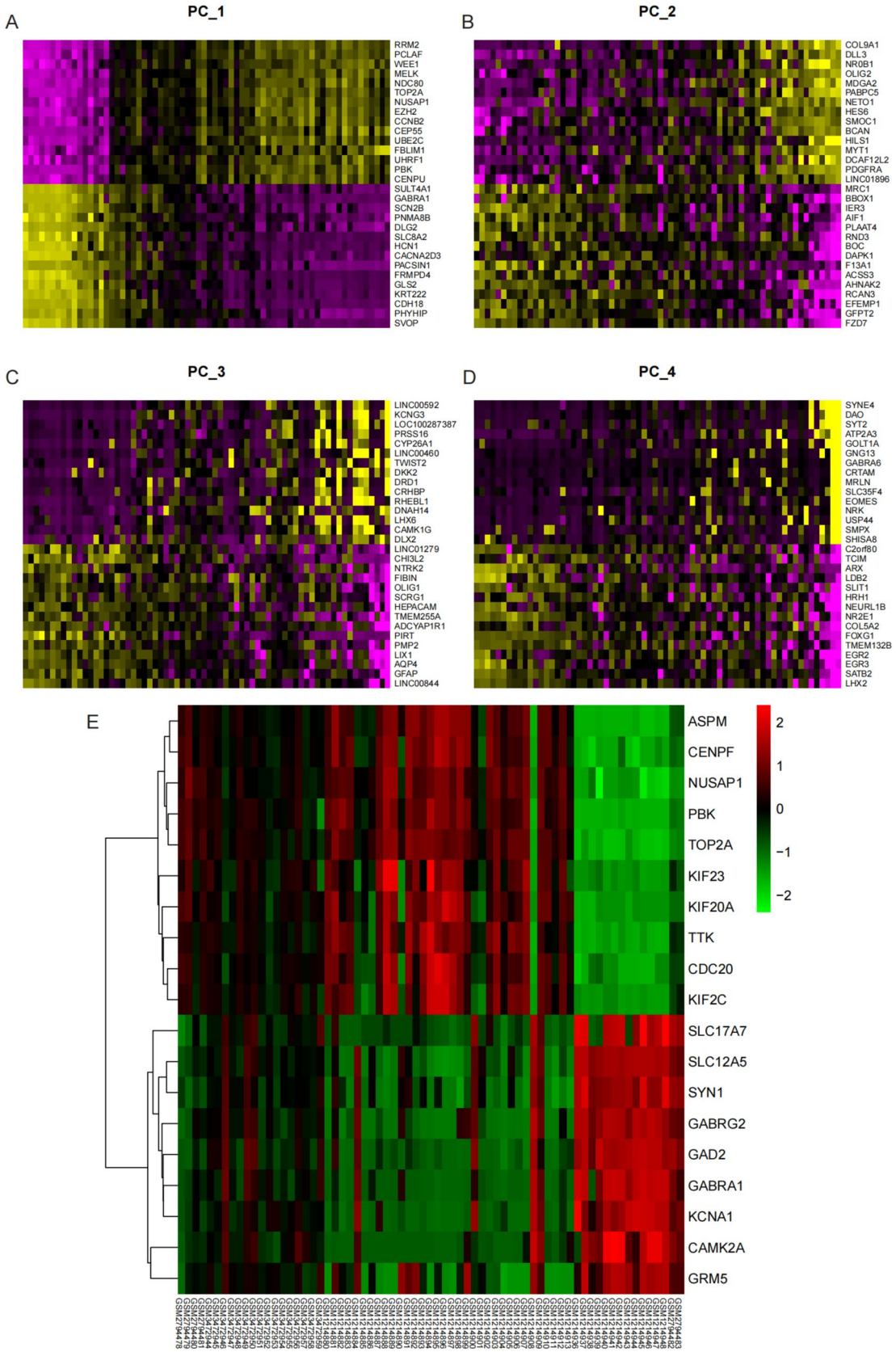

Fig. 8 Heat map of gene expression. Differential expression of core genes between glioma tumor and non-tumor samples

Core gene expression analysis

Through meticulous expression analysis, 10 genes crucial for brain glioma (CENPF, PBK, ASPM, KIF2C, KIF20A, CDC20, TOP2A, NUSAP1, TTK, KIF23) were found to be relatively highly expressed in tumor tissues. Statistical significance was achieved with a P-value less than 0.05 (Fig. 9).

CTD analysis

In this study, the CTD website was utilized by inputting the list of hub genes to probe for diseases associated with the core genes, thereby deepening the understanding of gene-disease associations. The 10 genes of focus (CENPF, PBK, ASPM, KIF2C, KIF20A, CDC20, TOP2A, NUSAP1, TTK, KIF23) were found to have potential correlations with multiple medical conditions.

Notably, connections to carcinomas, especially hepatocellular carcinoma, were identified. Dermatological implications were evident, with contact dermatitis being a prime example. There were also links to chemically/drug-induced liver injury and necrosis, suggesting impacts on hepatic cell viability. Hyperplasia, a potential precursor to cancer, was implicated, along with weight loss, potentially due to perturbed metabolic pathways. Inflammation, a ubiquitous factor in diseases, was involved, hinting at immune-modulating capabilities of these genes. Prenatal exposure-delayed effects underlined long-term consequences. Hepatomegaly and neoplasms, including experimental models, were associated, highlighting the genes' roles in tumorigenesis and organ pathology. Figure 10 visually captures these complex relationships, providing a foundation for further research into mechanisms and potential therapies (Fig. 10).

Prediction and functional annotation of miRNA associated with hub genes

Within the framework of this research endeavor, The Targetsacan platform was utilized by inputting the list of hub genes to explore relevant microRNAs (miRNAs), aiming to enhance the comprehension of gene expression regulation (Table 1). This investigation revealed specific miRNA

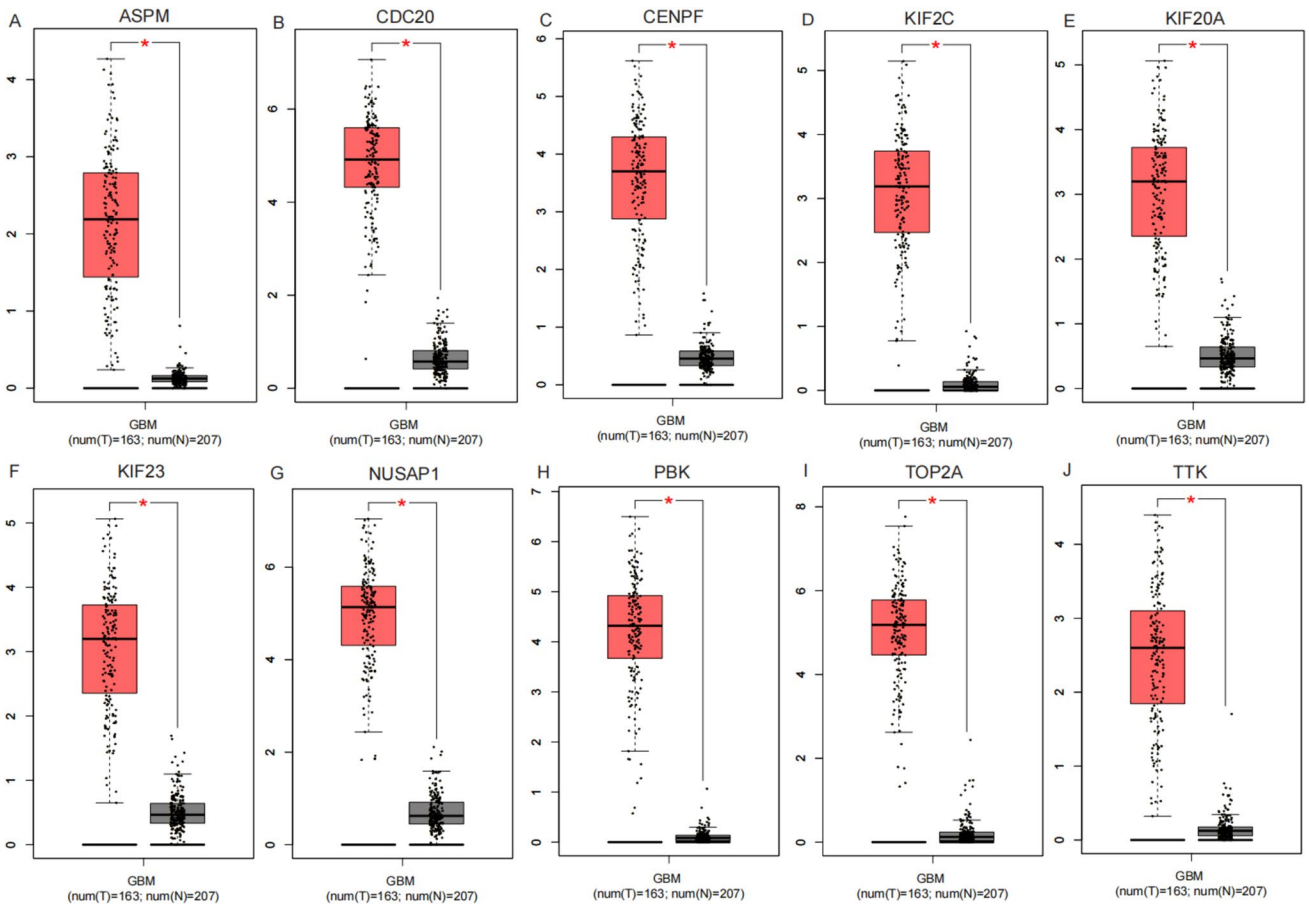

Fig. 9 Core gene expression analysis. Ten core genes related to glioma were relatively highly expressed in tumor tissues.**A** ASPM; **B** CDC20; **C** CENPF; **D** KIF2C; **E** KIF20A; **F** KIF23; **G** NUSAP1; **H** PBK; **I** TOP2A; **J** TTK

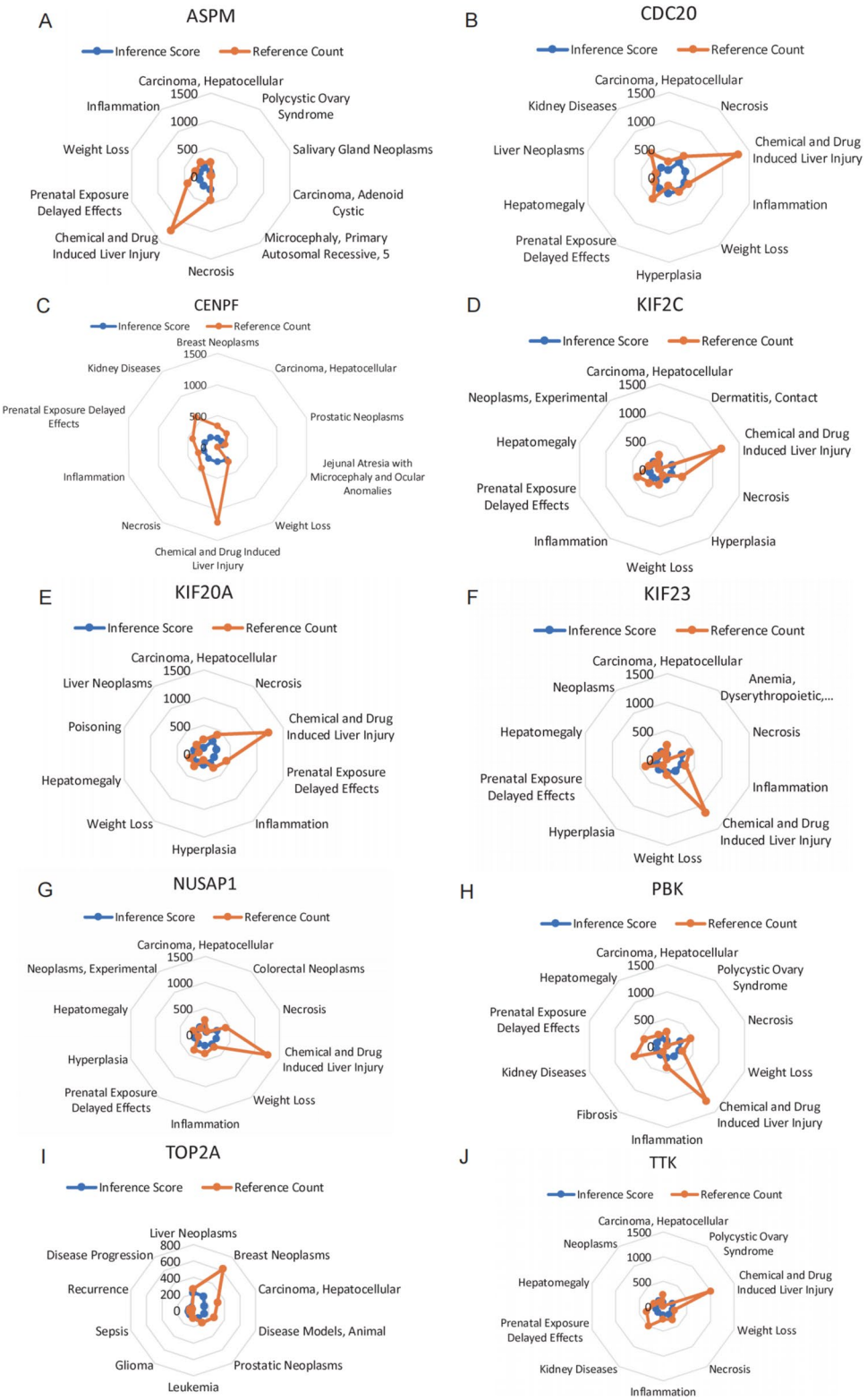

Fig. 10 Analysis of CTD. **A** ASPM; **B** CDC20; **C** CENPF; **D** KIF2C; **E** KIF20A; **F** KIF23; **G** NUSAP1; **H** PBK; **I** TOP2A; **J** TTK

associations for key genes. For the CENPF gene, the related miRNAs were identified as hsa-miR-302c-3p.2 and hsa-miR-520f-3p. In the case of the KIF20A gene, its associated miRNA was hsa-miR-153-3p. The TOP2A gene was found to be correlated with hsa-miR-144-3p, while the TTK gene was linked to hsa-miR-455-3p.1. Additionally, for the KIF23 gene, the associated miRNA is hsa-miR-103a-3p. These miRNA-gene relationships offer crucial insights

Table 1 A summary of miRNAs that regulate hub genes

	Gene	Predicted MiR	
1	CENPF	hsa-miR-302c-3p.2	hsa-miR-520f-3p
2	KIF20A	hsa-miR-153-3p	
3	TOP2A	hsa-miR-144-3p	
4	TTK	hsa-miR-455-3p.1	
5	KIF23	hsa-miR-103a-3p	hsa-miR-107

into the intricate regulatory mechanisms governing gene expression, potentially paving the way for future therapeutic interventions.

Immunofluorescence and western blot analysis

Immunofluorescence and western blot analysis elucidated a significant expression pattern in glioma. Notably, CENPF exhibited a high level of expression, while p53 was downregulated ($P < 0.05$). Concomitantly, both CENPF and CDK-1 were highly expressed, which was accompanied by a diminished expression of p53, p21, and Caspase 9. This coordinated alteration led to the suppression of the apoptotic pathway, consequently fueling glioma progression.

Upon overexpression of CENPF, the key components of the p53-mediated apoptotic pathway were further repressed. In contrast, when CENPF was underexpressed, these pivotal elements of the apoptotic pathway were activated, triggering apoptosis in glioma cells (Figs. 11, 12). Understanding these molecular dynamics provides a profound basis for deciphering glioma pathophysiology and paves the way for potential therapeutic manipulations.

Discussion

Glioma, representing the most prevalent primary malignant brain tumor, stems from the malignant transformation of glial cells within the brain and spinal cord. Tumor cells inflict severe physical harm by disrupting adjacent brain cells. And brain gliomas pose a formidable challenge in terms of curability and frequently recurring (Yang et al. 2022). Thus, delving deep into the molecular underpinnings of glioma is of paramount importance for the advancement of targeted drug research.

The cardinal finding of this study reveals that CENPF is highly expressed in glioma. This overexpression likely impedes cell apoptosis via the p53 signaling pathway, thereby facilitating the initiation and progression of glioma. Comprehending this molecular cascade not only enriches the understanding of glioma pathophysiology but also holds the potential to herald novel therapeutic strategies.

CENPF, also known as centromeric protein F, encodes a protein that plays a pivotal role in mitosis. It is indispensable for kinetochore functionality and accurate chromosome segregation, serving as a crucial nexus between recycling vesicles and microtubule networks to modulate plasma membrane recycling (Li et al. 2021). Functioning as a key regulator of chromosome partitioning, CENPF expression is intimately intertwined with the cell cycle. It exhibits a progressive accumulation throughout the cell cycle and undergoes degradation upon mitotic completion.

Deficiency of CENPF triggers a cascade of mitotic aberrations, ranging from spindle assembly failures and abnormal chromosomal alignment and segregation, to potentially culminating in cell death (Li et al. 2022). Moreover, CENPF is likely implicated in the regulatory

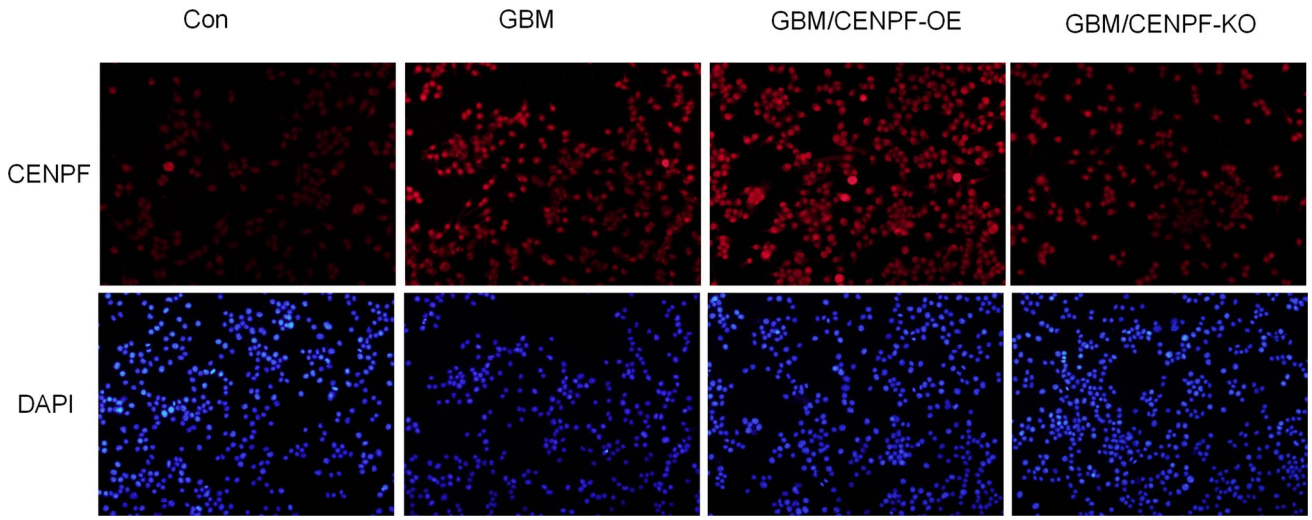

Fig. 11 Immunofluorescence analysis of CENPF

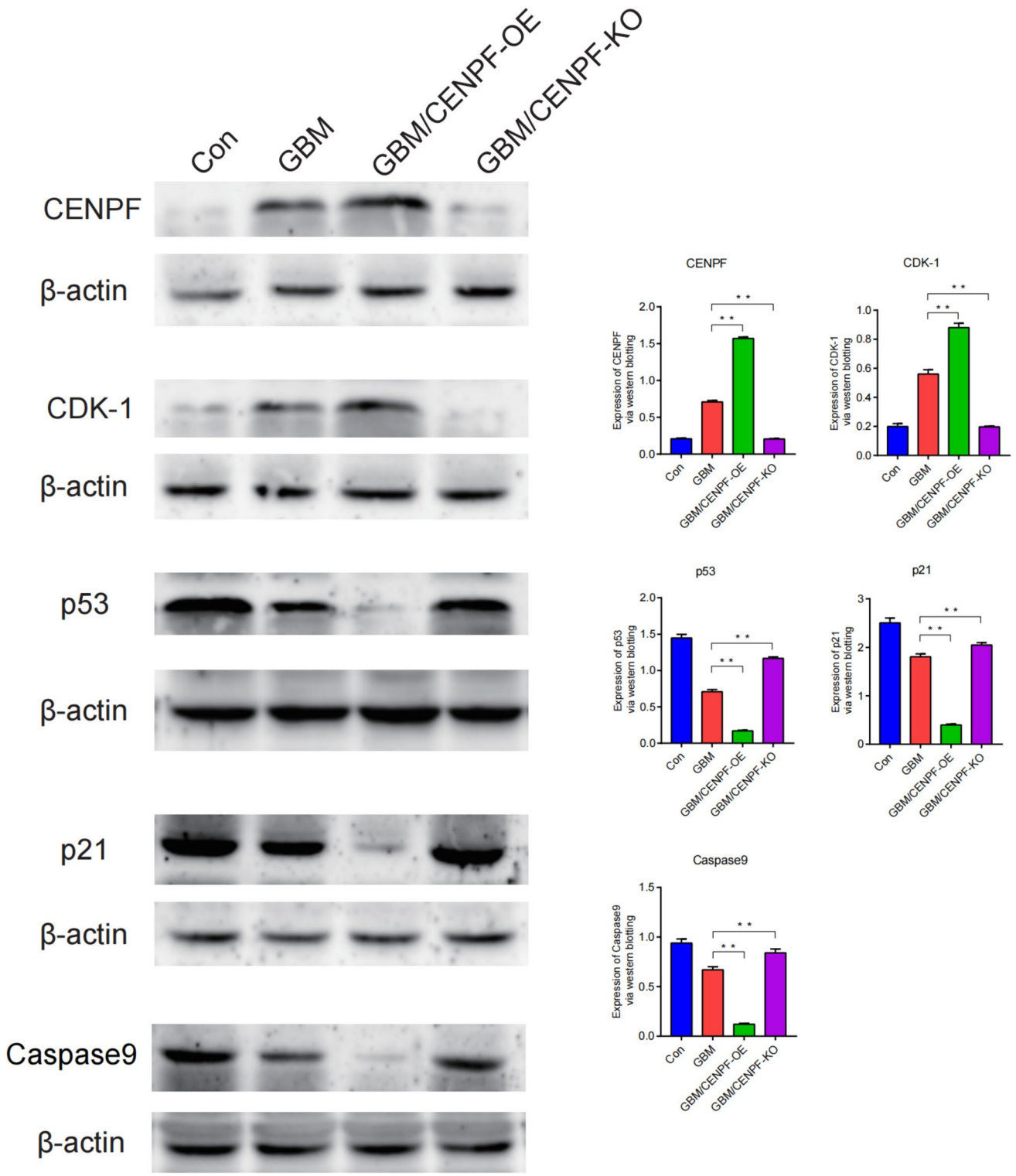

Fig. 12 Western blot analysis. CENPF, CDK-1, p53, p21, Caspase9. $P < 0.05$

dynamics of the Spindle Assembly Checkpoint (SAC), further highlighting its significance in maintaining genomic stability and the fidelity of cell division processes.

Centromere protein F (CENPF), a microtubule-binding protein, has been demonstrated to modulate cancer metabolism by governing the pyruvate kinase M2 phosphorylation signaling pathway (Shahid et al. 2018).

Furthermore, the study by Hongjin Chen et al. (Huang et al. 2021) unveiled that centromeric protein F, emerging as a novel genomic research-derived therapeutic target, plays a crucial part in the pathogenesis of pancreatic cancer. CENPF partakes in the regulation of DNA synthesis, thereby orchestrating cell cycle progression. Additionally, it functions as a cardinal regulator of cancer metabolism, potentially via its influence on mitochondrial function. Notably, its overexpression has been correlated with the onset of numerous human malignancies (Chen et al. 2024). Given these precedents, it is rationally postulated that CENPF occupies a central position in glioma progression, warranting further in-depth investigation to decipher its underlying mechanisms and explore potential therapeutic interventions.

p53, a quintessential tumor suppressor gene, encodes a transcriptional factor that exerts a pivotal role in governing the initiation of the cell cycle (Zhou et al. 2022). In the normal physiological state, akin to other tumor suppressors, the p53 gene functions as a sentinel, moderating and surveilling cell division processes. The p53 protein exhibits a characteristic distribution pattern, predominantly residing in both the nucleus and cytoplasm, endowing it with the capacity to specifically interact with DNA. Its functional activity is subject to intricate regulation via an array of post-translational modifications, including phosphorylation, acetylation, methylation, and ubiquitination (Zhang et al. 2020). The intracellular p53 gene, a key player in cancer inhibition, serves as a barometer for gauging the extent of DNA mutation. In scenarios where the mutation is relatively minor, p53 intervenes to impede DNA replication and triggers cellular self-repair mechanisms. Conversely, when confronted with extensive DNA mutations and failed repair attempts, p53 orchestrates apoptosis. Moreover, the p53 protein manifests its presence not only in the aforementioned compartments but also in mitochondria and the nucleolus, among other cellular structures, and engages in dynamic interactions with the cytoskeleton (Tu et al. 2020). Understanding these complex and nuanced functions of p53 provides a profound foundation for deciphering cancer biology and devising potential therapeutic strategies.

CENPF (Centromeric Protein F) is inextricably intertwined with the progression of glioma (Xu et al. 2023). The underlying mechanisms by which CENPF exerts its influence are multifaceted and principally encompass several key aspects: dysregulated cell-cycle control, chromosomal instability, the inhibition of cell apoptosis, modulation of the tumor microenvironment, and intricate crosstalk with relevant genes and signaling cascades (Lokody 2014). Notably, a complex regulatory relationship prevails between CENPF and p53, which is expounded in the following detailed analysis:

Cell-cycle regulation

CENPF, a protein intrinsically associated with the centromere - kinetochore complex, assumes a pivotal role in ensuring the precise segregation of chromosomes during the mitotic process. Its expression profile demonstrates a conspicuous peak during the G2/M phase of the cell cycle (Huang et al. 2022). On the other hand, p53, a critically important tumor-suppressor gene, is activated in response to diverse cellular stressors, such as DNA damage or other abnormal cellular states. Once activated, p53 orchestrates a series of regulatory events by modulating the expression of an array of cell-cycle-related proteins (Barnes et al. 2019). This ultimately leads to the arrest of the cell cycle at the G1, S, or G2/M phase, effectively halting the abnormal proliferation of cells (Sun et al. 2023).

Under certain pathophysiological conditions, the aberrant expression of CENPF can precipitate chromosomal segregation irregularities. These anomalies trigger the activation of intracellular stress-sensing mechanisms, which in turn initiate a cascade of events culminating in the activation of the p53 signaling pathway. Once engaged, the p53-mediated signaling cascade may act in a negative-feedback loop to suppress either the expression or the functional activity of CENPF. This negative regulation serves as a compensatory mechanism aimed at rectifying the disrupted cell-cycle dynamics. For instance, in the context of adrenocortical carcinoma, gene-set enrichment analysis (GSEA) has unequivocally demonstrated that CENPF is prominently involved in the G2/M-phase-mediated cell-cycle progression and the p53 signaling network. In vitro experimental evidence has further revealed that the interaction between CENPF and CDK1 significantly enhances the G2/M-phase transition during mitosis (Huang et al. 2022), promotes robust cell proliferation, and concurrently has the potential to evoke p53-mediated anti-tumor responses.

Tumorigenesis and tumor progression

CENPF has been consistently observed to exhibit elevated expression levels across a wide spectrum of tumors, including hepatocellular carcinoma (Li et al. 2021) and prostate cancer (Lin et al. 2016). This upregulated expression endows CENPF with the capacity to potently promote tumor-cell proliferation, migration, and invasion, thereby fueling the malignant progression of tumors.

In contrast, p53, in its normal, functional state, serves as a formidable guardian against tumorigenesis. It exerts its tumor-suppressive effects through a repertoire of well-characterized mechanisms, such as the induction of apoptosis

and the enforcement of cell-cycle arrest (Kastenhuber and Lowe 2017). However, when the p53 gene succumbs to mutation or deletion, a critical event occurs: the loss of its normal tumor-suppressive function (Aubrey et al. 2018). This loss of function effectively removes the inhibitory constraint on CENPF, allowing CENPF to act in an unregulated manner. As a consequence, CENPF can then drive the malignant biological behaviors of tumor cells, further promoting tumor progression.

Conversely, a functionally intact p53 can, through a complex network of molecular interactions, suppress the expression or activity of CENPF. This suppression represents a key regulatory mechanism that restricts tumor-cell proliferation and invasion, thereby curbing the overall progression of tumors (Liu et al. 2024). For example, in prostate cancer, a significant correlation has been established between the expression of CENPF and the degree of tumor progression, as well as poor prognosis (Lin et al. 2016). Similarly, mutations in the p53 gene have been firmly associated with the prognosis of multiple malignancies, including breast cancer (Marvalim et al. 2023). Mutated p53 not only contributes to the advancement of tumors but also confers chemoresistance, further highlighting the intricate and reciprocal relationship between CENPF and p53 in the complex landscape of tumor development.

Identifying CENPF as a prognostic marker for glioma could aid in risk stratification. High CENPF expression might indicate a poorer prognosis, guiding more aggressive treatment strategies (Li et al. 2022; Xu et al. 2023). Additionally, targeting the CENPF-p53 axis could be a novel therapeutic approach, potentially leading to the development of drugs that modulate this pathway to inhibit glioma growth (Song et al. 2024). Despite the implementation of a rigorous bioinformatics analysis framework within this study, certain limitations remain conspicuous. Notably, patient trials, which are pivotal for corroborating the functional implications unearthed, were regrettably absent. Absence of such empirical validation restricts the translational potential of the current findings. Future studies should focus on conducting patient trials to confirm the role of CENPF in glioma prognosis and treatment. Investigations into developing drugs that target the CENPF-p53 pathway are also needed. This could involve screening small molecules or biologics to modulate CENPF expression or its interaction with the p53 pathway, aiming to translate these findings into effective clinical treatments.

Conclusion

In conclusion, CENPF demonstrates potential as a prognostic marker for glioma. Elevated expression levels of CENPF in glioma may inhibit cell apoptosis via the p53 signaling pathway, thereby contributing to the onset and progression of the disease.

Author contribution X.Y. prepared all figures and tables. X.P.wrote the main manuscript text. X.P.Y. conduct experiments and analyze the data. All authors reviewed the manuscript.

Funding No external funding was used.

Data availability No datasets were generated or analysed during the current study.

Declarations

Conflict of interest The authors declare no conflicts of interest.

References

Agupitan AD, Neeson P, Williams S, Howitt J, Haupt S, Haupt Y (2020) P53: a guardian of immunity becomes its saboteur through mutation. Int J Mol Sci 21(10):3452. https://doi.org/10.3390/ijms21103452

Aubrey BJ, Kelly GL, Janic A, Herold MJ, Strasser A (2018) How does p53 induce apoptosis and how does this relate to p53-mediated tumour suppression? Cell Death Differ 25(1):104–113. https://doi.org/10.1038/cdd.2017.169

Barnes PJ, Baker J, Donnelly LE (2019) Cellular senescence as a mechanism and target in chronic lung diseases. Am J Respir Crit Care Med 200(5):556–564. https://doi.org/10.1164/rccm.201810-1975TR

Chen C, Hou J, Tanner JJ, Cheng J (2020) Bioinformatics methods for mass spectrometry-based proteomics data analysis. Int J Mol Sci 21(8):2873. https://doi.org/10.3390/ijms21082873

Chen H, Wang X, Wu F et al (2021) Centromere protein F is identified as a novel therapeutic target by genomics profile and contributing to the progression of pancreatic cancer. Genomics 113(1 Pt 2):1087-1095. https://doi.org/10.1016/j.ygeno.2020.10.039

Ellert-Miklaszewska A, Ciechomska IA, Kaminska B (2020) Cannabinoid signaling in glioma cells. Adv Exp Med Biol 1202:223–241. https://doi.org/10.1007/978-3-030-30651-9_11

Fu Y, Ling Z, Arabnia H, Deng Y (2020) Current trend and development in bioinformatics research. BMC Bioinform 21(Suppl 9):538. https://doi.org/10.1186/s12859-020-03874-y

Gusyatiner O, Hegi ME (2018) Glioma epigenetics: from subclassification to novel treatment options. Semin Cancer Biol 51:50–58. https://doi.org/10.1016/j.semcancer.2017.11.010

Huang Y, Chen X, Wang L, Wang T, Tang X, Su X (2021) Centromere protein F (CENPF) serves as a potential prognostic biomarker and target for human hepatocellular carcinoma. J Cancer 12(10):2933–2951. https://doi.org/10.7150/jca.52187

Huang YG, Li D, Wang L, Su XM, Tang XB (2022) CENPF/CDK1 signaling pathway enhances the progression of adrenocortical carcinoma by regulating the G2/M-phase cell cycle. J Transl Med 20(1):78. https://doi.org/10.1186/s12967-022-03277-y

Hur K, Jearn LH, Kim TY (2019) Centromere protein-F-like pattern in a patient with rheumatoid arthritis. Ann Lab Med 39(2):227–228. https://doi.org/10.3343/alm.2019.39.2.227

Kastenhuber ER, Lowe SW (2017) Putting p53 in context. Cell 170(6):1062–1078. https://doi.org/10.1016/j.cell.2017.08.028

Li R, Wang X, Zhao X et al (2020) Centromere protein F and Forkhead box M1 correlation with prognosis of non-small cell lung cancer. Oncol Lett 19(2):1368–1374. https://doi.org/10.3892/ol.2019.11232

Li X, Li Y, Xu A et al (2021) Apoptosis-induced translocation of centromere protein F in its corresponding autoantibody production in hepatocellular carcinoma. Oncoimmunology 10(1):1992104. https://doi.org/10.1080/2162402X.2021.1992104

Li M, Zhao J, Yang R et al (2022) CENPF as an independent prognostic and metastasis biomarker corresponding to CD4+ memory T cells in cutaneous melanoma. Cancer Sci 113(4):1220–1234. https://doi.org/10.1111/cas.15303

Lin SC, Kao CY, Lee HJ et al (2016) Dysregulation of miRNAs-COUP-TFII-FOXM1-CENPF axis contributes to the metastasis of prostate cancer. Nat Commun 7:11418. https://doi.org/10.1038/ncomms11418

Liu Y, Tavana O, Gu W (2019) p53 modifications: exquisite decorations of the powerful guardian. J Mol Cell Biol 11(7):564–577. https://doi.org/10.1093/jmcb/mjz060

Liu J, Cao L, Wang Y et al (2024) The phosphorylation-deubiquitination positive feedback loop of the CHK2-USP7 axis stabilizes p53 under oxidative stress. Cell Rep 43(6):114366. https://doi.org/10.1016/j.celrep.2024.114366

Lokody I (2014) Signalling: FOXM1 and CENPF: co-pilots driving prostate cancer. Nat Rev Cancer 14(7):450–451. https://doi.org/10.1038/nrc3772

Marvalim C, Datta A, Lee SC (2023) Role of p53 in breast cancer progression: an insight into p53 targeted therapy. Theranostics 13(4):1421–1442. https://doi.org/10.7150/thno.81847

Norouzi M (2020) Gold nanoparticles in glioma theranostics. Pharmacol Res 156:104753. https://doi.org/10.1016/j.phrs.2020.104753

Sabapathy K, Lane DP (2019) Understanding p53 functions through p53 antibodies. J Mol Cell Biol 11(4):317–329. https://doi.org/10.1093/jmcb/mjz010

Shahid M, Lee MY, Piplani H et al (2018) Centromere protein F (CENPF), a microtubule binding protein, modulates cancer metabolism by regulating pyruvate kinase M2 phosphorylation signaling. Cell Cycle 17(24):2802–2818. https://doi.org/10.1080/15384101.2018.1557496

Song B, Yang P, Zhang S (2024) Cell fate regulation governed by p53: friends or reversible foes in cancer therapy. Cancer Commun (Lond) 44(3):297–360. https://doi.org/10.1002/cac2.12520

Sun X, Klingbeil O, Lu B et al (2023) BRD8 maintains glioblastoma by epigenetic reprogramming of the p53 network. Nature 613(7942):195–202. https://doi.org/10.1038/s41586-022-05551-x

Tang J, Kong D, Cui Q et al (2018) Prognostic genes of breast cancer identified by gene co-expression network analysis. Front Oncol 8:374. https://doi.org/10.3389/fonc.2018.00374

Tsitlakidis A, Aifantis EC, Kritis A et al (2020) Mechanical properties of human glioma. Neurol Res 42(12):1018–1026. https://doi.org/10.1080/01616412.2020.1796381

Tu Y, Chen L, Ren N et al (2020) Standardized saponin extract from Baiye No.1 Tea (Camellia sinensis) flowers induced s phase cell cycle arrest and apoptosis via AKT-MDM2-p53 signaling pathway in ovarian cancer cells. Molecules 25(15):3515. https://doi.org/10.3390/molecules25153515

Xu S, Tang L, Li X, Fan F, Liu Z (2020) Immunotherapy for glioma: current management and future application. Cancer Lett 476:1–12. https://doi.org/10.1016/j.canlet.2020.02.002

Xu P, Yang J, Chen Z et al (2023) N6-methyladenosine modification of CENPF mRNA facilitates gastric cancer metastasis via regulating FAK nuclear export. Cancer Commun (Lond) 43(6):685–705. https://doi.org/10.1002/cac2.12443

Yang K, Wu Z, Zhang H et al (2022) Glioma targeted therapy: insight into future of molecular approaches. Mol Cancer 21(1):39. https://doi.org/10.1186/s12943-022-01513-z

Zhang LZ, Yang JE, Luo YW, Liu FT, Yuan YF, Zhuang SM (2020) A p53/lnc-Ip53 negative feedback loop regulates tumor growth and chemoresistance. Adv Sci (Weinh) 7(21):2001364. https://doi.org/10.1002/advs.202001364

Zhou S, Han H, Yang L, Lin H (2022) MiR-1–3p targets CENPF to repress tumor-relevant functions of gastric cancer cells. BMC Gastroenterol 22(1):145. https://doi.org/10.1186/s12876-022-02203-2